Polypropylene-Dispersed Domain as Potential Nucleating Agent in PS and PMMA Solid-State Foaming

Rahida Wati Sharudin, Abacha Nabil, Kentaro Taki, Masahiro Ohshima

Department of Chemical Engineering, Kyoto University, Kyoto 615-8510, Japan

ABSTRACT: The potential of using dispersive domains in a polymer blend as a bubble nucleating agent was investigated by exploiting its high dispersibility in a matrix polymer in the molten state and its immiscibility in the solid state. In this experiments, polypropylene (PP) was used as the nucleating agent in polystyrene (PS) and poly(methyl methacrylate) (PMMA) foams at the weight fraction of 10, 20, and 30 wt %. PP creates highly dispersed domains in PS and PMMA matrices during the extrusion processing. The high diffusivity of the physical foaming agent, i.e., CO_2 in PP, and the high interfacial tension of PP with PS and PMMA could be beneficial for providing preferential bubble nucleation sites. The experimental results of the pressure quench solid-state foaming of PS/PP and PMMA/PP blends verified that the dispersed PP could successfully increase the cell density over 10^6 cells/cm^3 for PS/PP and 10^7 cells/cm^3 for PMMA/PP blend and reduce the cell size to 24 μm for PS/PP and 9 μm for PMMA/PP blends foams. The higher interfacial tension between PP and the matrix polymer created a unique cell morphology where dispersed PP particles were trapped inside cells in the foam. © 2010 Wiley Periodicals, Inc. J Appl Polym Sci 119: 1042–1051, 2011

Key words: bubble nucleation; polymer blend; solid-state foaming; supercritical carbon dioxide

INTRODUCTION

Although various new foam products have been developed recently, improving the cell structure is still important because smaller and more uniform cells can provide good mechanical properties[1–3] as well as significant reduction of the amount of plastics materials.[4] Fine cell structure and high cell density have been shown to be dependent on the bubble nucleation rate in polymers. The nucleation of bubbles can take place via two mechanisms: one is homogeneous and the other heterogeneous.[5] Nucleating agents, such as talc and nanoclay, can be used to induce heterogeneous nucleation for producing a large number of nucleation sites. The addition of a nucleating agent increases the bubble nucleation rate, which enables better control of the cell morphology, cell density, cell size, and cell size distribution. The effect of nucleating sites on the cell morphology may depend on the type and size of the nucleating agent.[6] Small-sized and uniformly distributed particles in a polymer matrix would be the most suitable nucleating agents for producing high cell density and small cell size in polymeric foams. There have been many reports on the use of inorganic particle as nucleating agents. In the last decade, the use of nanosized inorganic particles has been investigated. Zhai et al.[7] indicated that nanosilica aggregates dramatically increased the bubble nucleation rate in PC/nanosilica composites. A pioneering study investigating the use of nanoclay as a bubble nucleating agent in polymer foam was reported by Nam et al.[8] They found that the addition of nanoclay to polypropylene (PP) drastically reduced the cell size and increased the cell density in PP foam. However, the use of inorganic materials as nucleating agents, especially nanosized particles such as nanoclay, creates difficulty in terms of dispersibility in the polymer. Organic modification on the surface of inorganic nucleating agents may improve the dispersion, but it reduces the performance of the nucleating agent. Taki et al.[9] pointed out that the bubble nucleation could not be drastically improved, but the bubble growth rate was suppressed to keep the cell size small by the addition of an organomodified nanoclay into polymer. The nucleating agent must be uniformly dispersed in the polymer matrix and provide a heterogeneous interface for bubble nucleation. However, both are often competitive and difficult to achieve at the same time.[9,10] An organic nucleating agent could be well dispersed at high temperatures by melt mixing, but

it would be immiscible and segregated from the matrix polymer at lower temperatures, so it could be used as an efficient nucleating agent by designing the appropriate processing conditions. Spitael et al.[11] reported that micelles with a polydimethylsiloxane (PDMS) core component increase the cell density in blend foaming, whereas polystyrene-b-poly (ethylene propylene) and PS-b-PMMA diblocks were not effective as a nucleating agent. They attributed the improvement in the cell density to the size of the micelles, which is near the critical bubble size, the aggregation of micelles, and the high surface tension of the core components. Ramesh et al.[12] studied the effect of a rubber component on the heterogeneous nucleation in high-impact PS foams. They claimed that existing microvoid in rubber could enhance the bubble nucleation. Recently, Nemoto et al.[13] controlled the bubble nucleation sites and size in PP/rubber blends and prepared a nanocellular foam by using their blend morphology as a template for bubble nucleation where the rubber domain plays the role of bubble nucleating site.

In this study, the potential of using a dispersive polymer domain in blend polymer as a bubble nucleating agent was investigated by exploiting its dispersibility of domain polymer in the matrix polymer in the molten state and its immiscibility in the solid state. We investigated PP as a bubble nucleating agent in polymer blend foams. PP is easily obtained, and its dispersibility in other polymers can be controlled by viscosity and temperature. Because of the higher solubility and diffusivity of CO_2 and N_2, which are often used as physical foaming agents, PP can also be used as a CO_2 reservoir and releaser. Furthermore, PP possesses high interfacial tension with other polymers such as PS and PMMA. Thus, PP can be used as an efficient bubble nucleating agent if the foaming conditions are chosen appropriately. Several experiments on the pressure quench batch foaming in solid-state PS/PP and PMMA/PP polymer blends were conducted to observe the effect of PP-dispersed domains on the cell density, cell size, and cell structure. This study focused especially on the relationship between the cell morphology and interfacial tension of PP with PS and PMMA.

EXPERIMENTAL

Materials

Homo-polypropylene (PP, M_w = 410,000) was supplied by Mitsubishi Chemical. Polystyrene (PS, M_w = 192,000) and poly(methyl methacrylate) (PMMA, M_w = 120,000) were obtained from Aldrich Chemical. All polymers were used as received.

Blend sample preparation

The PS/PP and PMMA/PP blends were prepared with a twin-screw extruder (ULT nano05, TECHNOVEL, Japan) at various blend ratios. The details of the processing scheme are as follows. Polymer resins were dry-blended before being fed into the hopper. Blending was carried out by twin screws, and the polymer resins were compounded at 220°C for 5 min. The screw rotor speed was kept constant at 38 rpm during the extrusion process. The extrudate was then grinded and compression-molded into a disc-shaped sample, 25 mm in diameter and 1 mm in thickness, using a hot press at 200°C and 10 MPa for 10 min.

Foaming process

The polymer samples were foamed by a pressure quench method. Samples were first placed in a pressure vessel and heated to the desired temperature. When the temperature reached the desired level, the autoclave was pressurized by CO_2 at a given pressure, and the samples were saturated with supercritical carbon dioxide (scCO$_2$) for 6 h. After a predetermined sorption time, scCO$_2$ in the pressure vessel was released from the saturation pressure to ambient pressure within 10 s. Samples were then removed from the vessel, and the cell structure of the foamed samples was analyzed by SEM (Tiny-SEM, Technex, Japan). The cell density and cell size were determined from the SEM images with the aid of a software program (Image J). The number of cells per unit volume of foamed sample is determined by

$$N_f = [nM/A]^{3/2},$$

where n is the number of cells in a micrograph, A is the area of the micrograph, and M is the magnification factor.

The average diameter was calculated by manually measuring the diameter of at least 100 cells on the micrographs. For the cell diameter measurements, the standard deviation is also calculated.

Rheological characterization

The dynamic storage modulus, G', of each polymer as a function of strain rate was evaluated using a rheometer (ARES). A dynamic temperature ramp test was performed in a rectangular torsion mode in a temperature range from 30 to 200°C. The strain percentage was 10% in the temperature range from 30 to 100°C, 2% for 140 to 160°C, and reduced to 0.1% for 160 to 200°C. The heating rate was 2°C/min at every temperature.
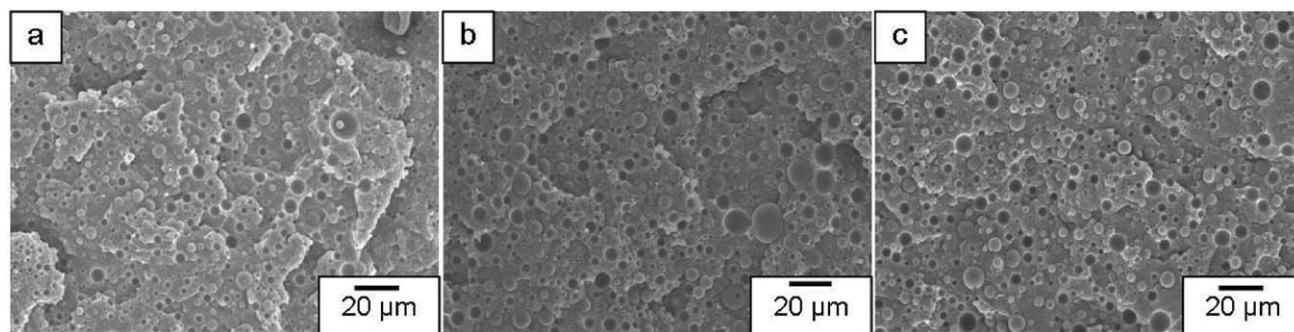
Figure 1 SEM micrographs of PS/PP blend morphology at different PP content; (a) 90/10; (b) 80/20, and (c) 70/30.

RESULT AND DISCUSSION

Blend morphology of PS/PP blend

Figure 1 shows the blend morphology of PS/PP at different blend ratios: 90/10, 80/20, and 70/30. In every PS/PP sample, a sea and island morphology, which has spherical-shaped dispersive domain of PP in the PS matrix, was observed. As the PP content increased, the number of PP spherical domain increased, while the average diameter of the domain remained about 4 μm as listed in Table I.

Effect of foaming condition on PS/PP cell structure

To investigate the effect of foaming temperature, batch foaming experiments were conducted on the PS/PP (80/20) blend at different foaming temperatures, 80, 100, and 120°C, and at a given saturation pressure of 15 MPa. The resulting cell structures are illustrated in Figure 2. The temperature dependence was clearly observed in the cell structures; the cell densities of the PS/PP blends foamed at 100 and 120°C were lower than that of the PS/PP foamed at 80°C. With the increase of foaming temperature, PP/PS blend foam shows the decrease in cell density. As the foaming temperature increases, the diffusivity of CO_2 in polymer increases and the viscosity of the polymer matrix decreases. At high temperature, polymer molecule has high mobility and allows CO_2 to diffuse into the growing bubbles rapidly. Then, the cell growth rate is increased by the increase in the diffusion rate. As a result, the bubbles grow faster and create cells of larger size at high foaming temperatures. Furthermore, bubbles coalescence rate increases at the temperatures above T_g of PS. The increase in bubble coalescence rate makes the cell size larger.

The saturation pressure and pressure release rate have considerable influence on the cell density, which could be observed in Figure 3. It shows the SEM images of PS/PP (80/20) foams prepared at the same temperature, 100°C, but different sorption levels of 8, 10, and 15 MPa. The pressure was released within 10 s. Thus, the pressure release rates were approximated to be 0.8, 1, and 1.5 MPa/s for each experiment. It has been reported that the increase in the saturation pressure resulted in a higher cell density.[14] The increase in the saturation pressure resulted in a higher solubility of CO_2 in polymer and a higher cell density. The high concentration of CO_2 in polymer would increase bubble nucleation rate. In Figure 3, it is clearly seen that PS/PP foams obtained at higher saturation pressure attained a much smaller cell size with higher cell density.

The effect of the pressure release rate on the PS/PP bubble density and cell size can be clearly seen in Figure 4. The PS/PP (80/20) foams were prepared by changing the pressure release rate while keeping the foaming temperature at 100°C and the saturation pressure at 10 MPa. The cell density decreased, and the cell size increased with the decrease in the pressure release rate. Table II summarizes the experimental data of cell size and density of PS/PP foams at various foaming conditions. The results concur with those in the previous studies,[9–16] i.e., a lower foaming temperature, higher saturation pressure, and higher depressurization rate lead to a higher cell density with a smaller cell size.

Effect of PP content on PS/PP blend foams

The influence of PP-dispersed domain on PS foams was investigated by foaming both neat PS and PS/PP blends. Figure 5 illustrates the SEM micrographs and histograms of the cell size distribution of both neat PS and PS/PP blend foams with different blend ratios. They were foamed by the pressure quench method at the same pressure and temperature

TABLE I
Average diameter of PP-dispersed domain

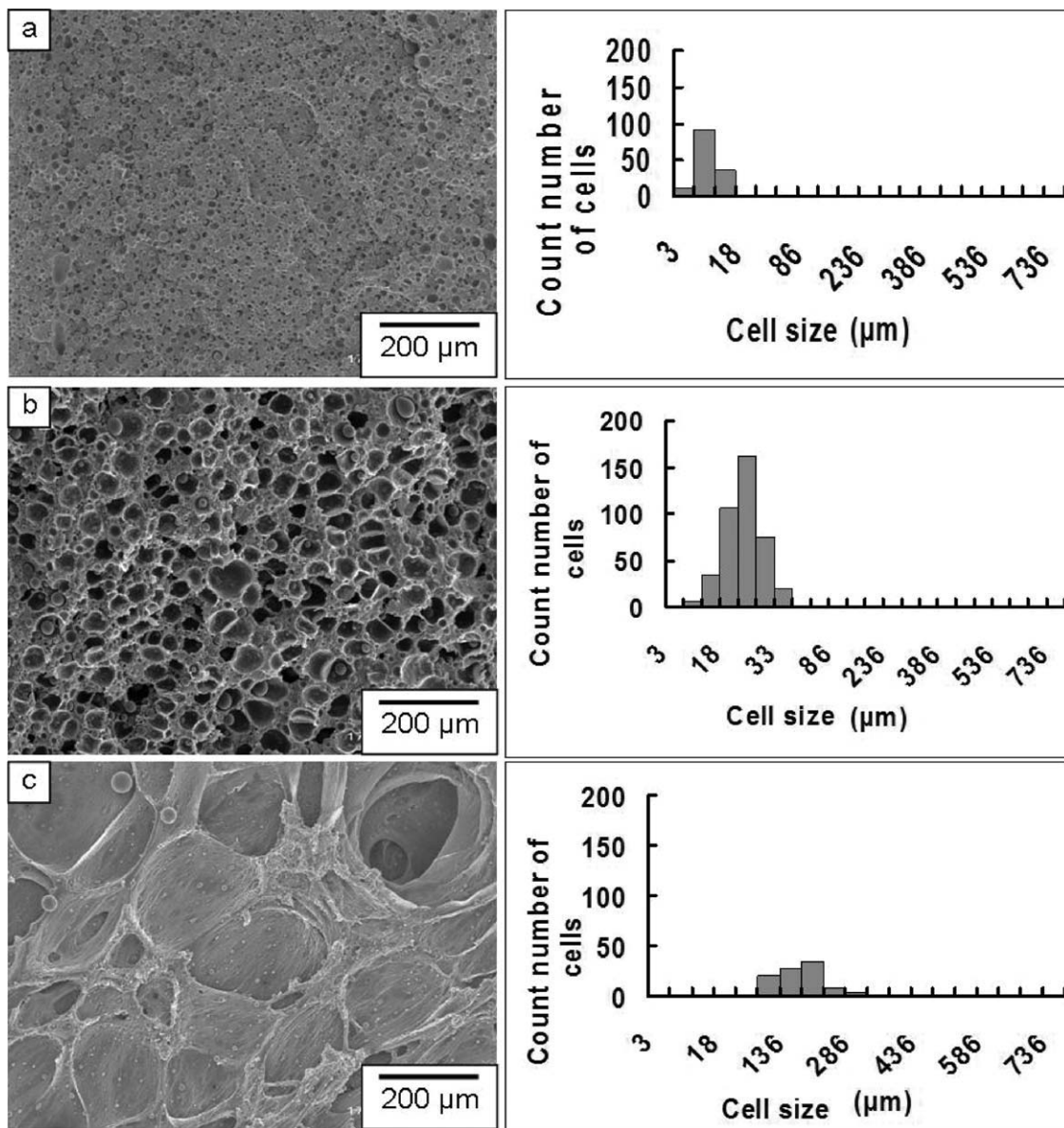| Blend ratio (PS/PP)	d_v of PP in PS/PP blend (μm)	d_v of PP in PMMA/PP blend (μm)
70/30	3.9 ± 1.3	8.6 ± 4.2
80/20	3.8 ± 1.9	6.0 ± 2.6
90/10	3.5 ± 0.8	3.1 ± 1.4

Figure 2 SEM images and cell size distribution of PS/PP foams at; (a) 80°C (b) 100°C, and (c) 120°C.

condition, i.e., 10 MPa and 100°C. The resulting cell structure of the PS/PP blend was quite different from that of the PS homopolymer foam. The uniformity of cell size was increased by the addition of PP. The cell size of the PS foam shows a broad distribution with cell size in a range from 13 to 78 μm. On the other hand, the cell size distribution of the PS/PP blend foams becomes narrower than that of
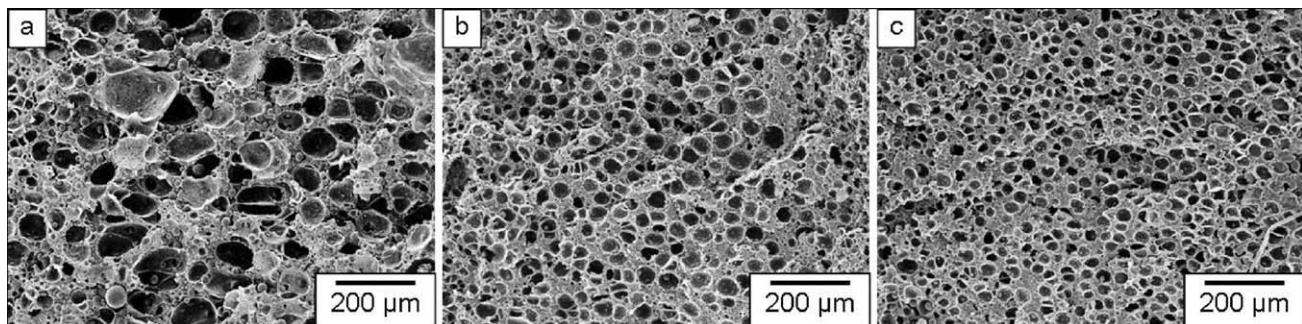

Figure 3 Cell morphologies of PS/PP (80/20) foams at 100°C and depressurization rate of 10 MPa/s. Saturation pressure: (a) 8 MPa; (b) 10 MPa; and (c) 15 MPa.
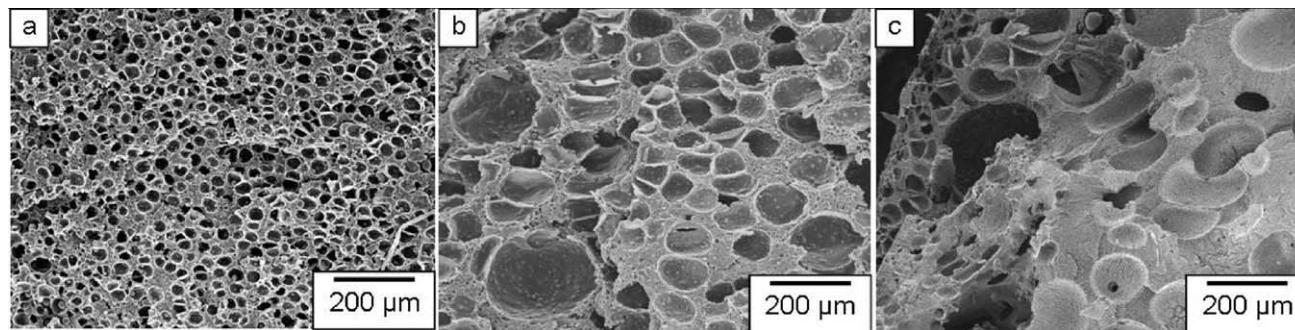
Figure 4 Cell morphologies of PS/PP (80/20) foams at 100°C and saturation pressure of 15 MPa. Pressure release time: (a) 10 s; (b) 120 s; and (c) 300 s.

neat PS foam, and they are in a range from 11 to 48 μm.

In addition to the improvement in the uniformity of cell size, an increase in the cell density was clearly observed in all PP contents over the PS homopolymer. It could be said that the presence of PP domains enhanced the bubble nucleation and suppressed the bubble growth. This is because the increase in the interfacial area between PS and PP could enhance the heterogeneous bubble nucleation at the interface between two polymers and increase the cell density. These results indicated the feasibility of PP as a nucleating agent for PS solid-state foaming.

Figure 5(b–d) shows that all the blend ratios have a similarly unique cell structure, wherein PP particles were surrounded by empty space and located inside the cells. The formation mechanism of this unique cell structure will be described further in the discussion section. The PP-dispersed domains remained as non-foamed particle because of its high stiffness and hard to foam at 100°C. It is highly possible that the strong suppression for the bubble nucleation in the PP domain was originated from the higher stiffness and

higher viscoelasticity of PP at this foaming temperature, which is illustrated in Figure 6. The higher elasticity increases the energy barrier for bubble nucleation and results in suppression of foaming.

Foaming behavior of PMMA/PP blends

The foaming experiments with PMMA/PP blends were also conducted to verify the role of the PP domains in polymer blend foaming. PMMA/PP blends were prepared with different blend ratios of 90/10, 80/20, and 70/30. Their blend morphologies were characterized before foaming, as the morphologies of the PS/PP blends had been. The effect of PP content on the morphology of PMMA/PP blends is illustrated in Figure 7. For all PP contents, a sea and island morphology was observed. However, when the PP content increased over 10 wt %, the dispersed PP domains coalesced. Large nonspherical PP domains were observed when the PP content was 30 wt %, as illustrated in Figure 7(c). These morphologies showed that the PMMA/PP blend is an incompatible polymer pair, and the PP domain size increases with increasing PP content.

TABLE II
Summary of the cell properties of PS/PP foams at various foaming conditions

| Sample	PP content (wt %)	Foaming condition			Cell density (10^6 cells/cm^3)	Average cell size (μm)
		T (°C)	P (MPa)	Depressurization (dp) time (s)		
Effect of PP content						
PS/PP	10	100	10	10	6.94	31.5 ± 18.3
PS/PP	20	100	10	10	12.30	25.9 ± 8.2
PS/PP	30	100	10	10	16.00	23.9 ± 8.1
Effect of foaming temperature						
PS/PP	20	80	15	10	138.00	9.14 ± 2.7
PS/PP	20	100	15	10	29.70	22.2 ± 4.9
PS/PP	20	120	15	10	0.45	178.5 ± 107.2
Effect of saturation pressure						
PS/PP	20	100	8	10	1.59	50.6 ± 18.3
PS/PP	20	100	10	10	12.30	25.9 ± 8.2
PS/PP	20	100	15	10	29.70	22.2 ± 4.9
Effect of pressure release time						
PS/PP	20	100	10	10	12.30	25.9 ± 8.2
PS/PP	20	100	10	120	1.82	49.2 ± 20.7
PS/PP	20	100	10	300	1.54	119.7 ± 62.7
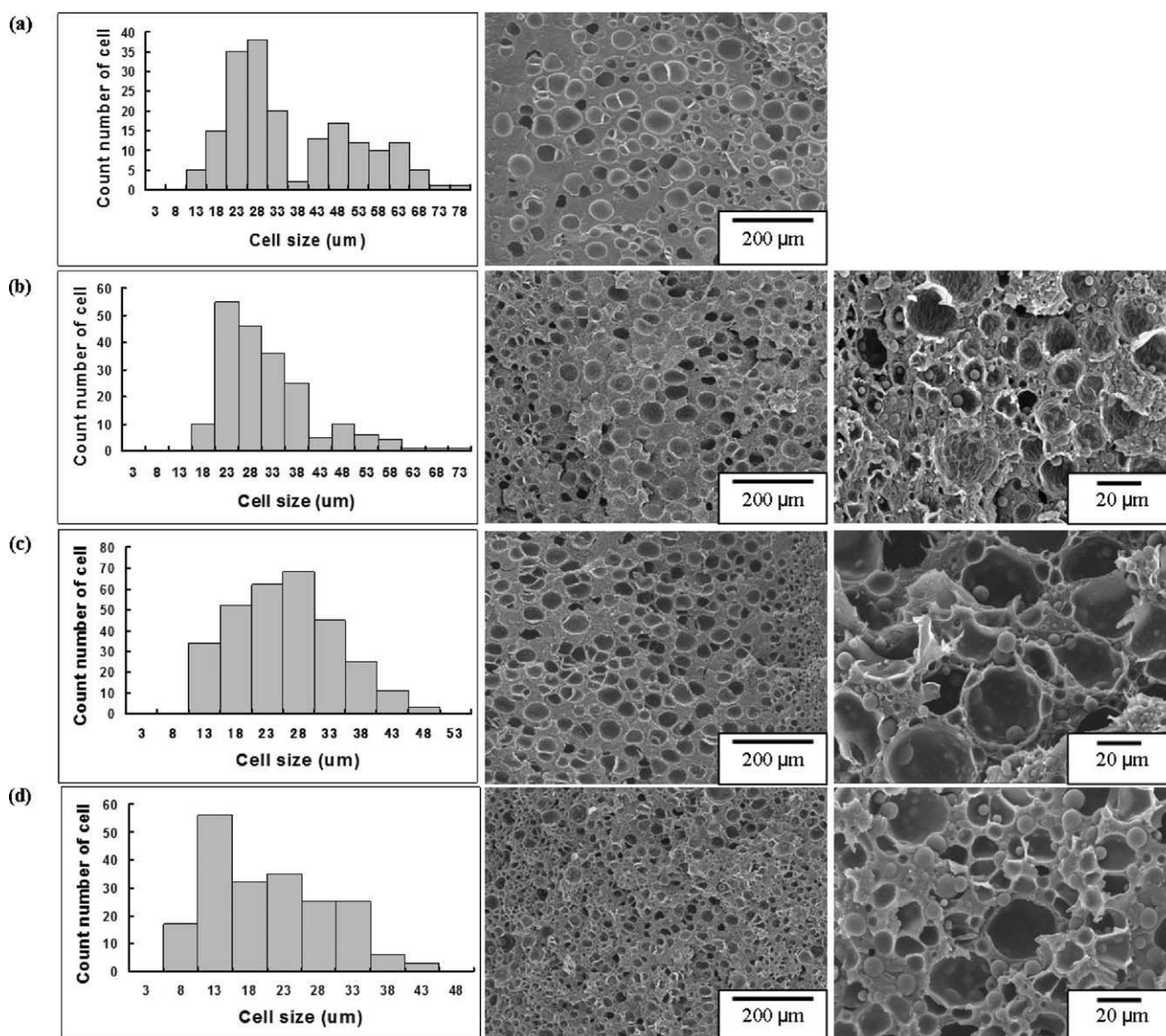
Figure 5 SEM micrographs and cell size distribution of samples foamed at 100°C, 10 MPa and depressurized at 1 MPa/s; (a) PS homopolymer, (b) PS/PP (90/10) blend, (c) PS/PP (80/20) blend, and (d) PS/PP (70/30) blend.

According to Calvao et al.,[17] coalescence occurs because of the high interfacial tension and the large viscosity ratio of the two polymers in a blend system.
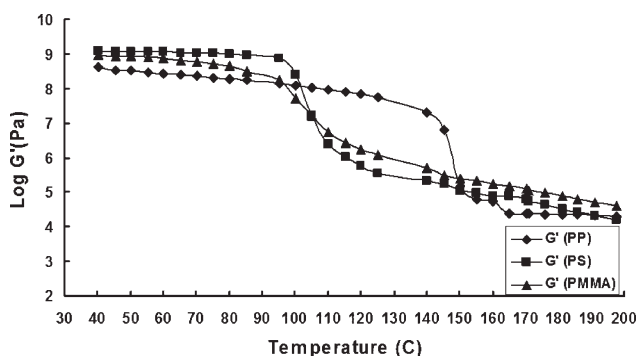

Figure 6 Storage modulus of PP, PS and PMMA homopolymers at different temperatures.

Figures 8 and 9 show the PMMA/PP (70/30) cell structures obtained for different foaming conditions: one was foamed at 80°C with a saturation pressure of 15 MPa, and the other was foamed at 100°C with a pressure of 10 MPa. The cell morphology of the dispersed PP domains enclosed by cells in the PS matrix was also observed in all PMMA/PP blends, as shown in Figures 8(d–f) and 9(d–f). To show the effect of PP content on cell density in PS/PP and PMMA/PP blend foams, the cell densities of the neat PS and PMMA foams as well as PS/PP and PMMA/PP blend foams are plotted against the PP content. Figures 10 and 11, respectively, show the plots of the cell density of the PS/PP and the PMMA/PP blend foams against the PP content. The cell density of the PS/PP blend foam increased with the increase in the PP content while it showed a
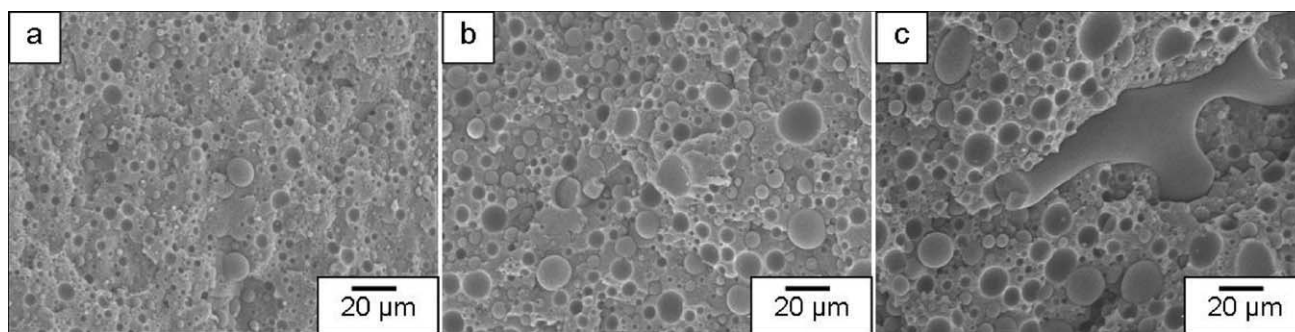
Figure 7 SEM micrographs of PMMA/PP blend morphology at different PP content; (a) 90/10; (b) 80/20; and (c) 70/30.

maximum value at 10% of PP content in PMMA/PP blend foam. The dispersed PP domains increased the cell density in PMMA/PP blend with 10 wt % of PP content. However, a drop in cell density with increasing PP content was observed in PMMA/PP blends over a 10 wt % blend ratio of PP. This reduction was caused by the coalescence of PP domains.

Discussion

An improvement in the cell density and cell size reduction was observed in PS/PP and PMMA/PP blends compared with homopolymers. The presence of PS/PP and PMMA/PP interfaces could be effectively reduce the activation energy barrier to bubble nucleation, thereby increasing the bubble nucleation rate. PP could be considered as a nucleating agent because it possesses the characteristic necessary for providing heterogeneous nucleation sites because of its higher interfa-

cial tension in the matrix polymer and function as a CO_2 reservoir. It was also observed that the presence of PP-dispersed domain created a unique cell structure, where PP particles were surrounded by empty space and located inside cells. The cell structure was the consequence of weak adhesion between two polymers in blend. CO_2 could easily diffuse into the interface and exfoliate the disperse domain from continuous phase. The interfacial tension between PMMA/PP is 7.5 mN/m and PS/PP is 5.68 mN/m[18] as listed in Table III. Higher interfacial tension means that a large surface energy is needed to create the interface, and thus the adhesion between two polymers is so low. As a result, at the interface with higher interfacial tension, CO_2 easily diffuses and expands the space between the two polymer interfaces. From the viewpoint of bubble nucleation theory, the relationship between the high interfacial tension of blend polymers and the bubble nucleation can be explained
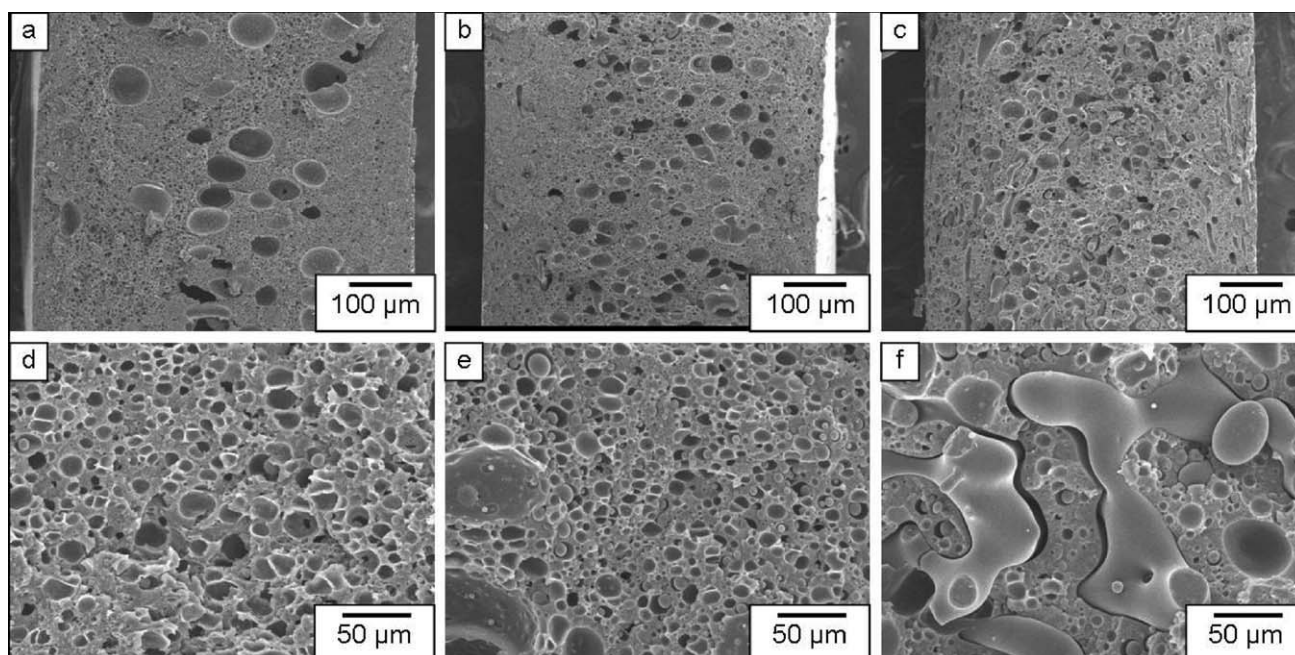

Figure 8 SEM images of PMMA/PP foams at 80°C and 15 MPa. Blend ratio: (a) and (d) 90/10; (b) and (e) 80/20; and (c) and (f) 70/30.
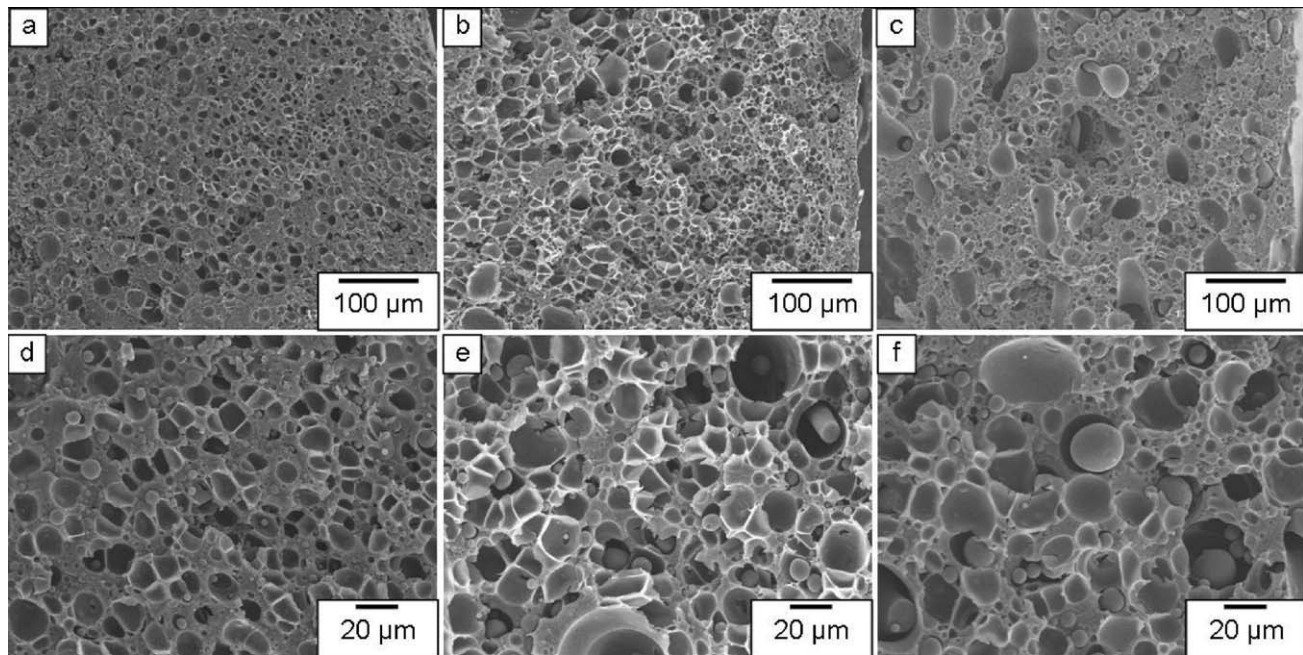
Figure 9 SEM images of PMMA/PP foams at 100°C and 10 MPa. Blend ratio: (a) and (d) 90/10; (b) and (e) 80/20; and (c) and (f) 70/30.

by Blander's model. Blander proposed a thermodynamics model of bubble nucleation at an interface between two immiscible liquids.[19] The bubble nucleation rate, J, was described as:

$$J = C \exp\left[\frac{-16\pi\gamma^3\Theta}{3kT\Delta P^2}\right],$$

where C is pre-exponential, γ is surface tension, and Θ is the contact angle of the bubble on the nucleating surface.

$$\Theta = \frac{1}{4\gamma_A^3}\left\{\gamma_A^3\left(2 - 3m_A + m_A^3\right) + \gamma_B^3\left(2 - 3m_A + m_A^3\right)\right\}$$

$$m_A = \cos(\pi - \theta) = \frac{\gamma_A^2 + \gamma_{AB}^2 - \gamma_B^2}{2\gamma_A\gamma_{AB}}$$

$$m_B = \cos(\pi - \phi) = \frac{\gamma_B^2 + \gamma_{AB}^2 - \gamma_A^2}{2\gamma_B\gamma_{AB}}.$$

Based on these nucleation equations, a generalization can be made with respect to the change in the bubble nucleation sites by the relative values of the various interfacial tensions, as illustrated in Figure 12.

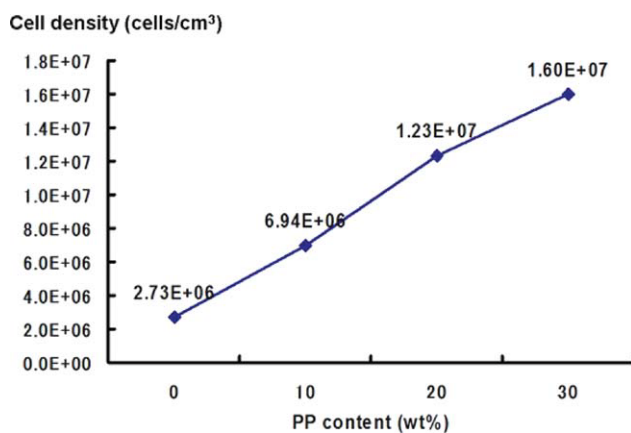(1) In the case of $\gamma_B \geq \gamma_A + \gamma_{AB}$, less energy is required to form a bubble in polymer A.

Figure 10 Plots of cell density of PS homopolymer and PS/PP blends at different PP content foamed at 100°C and 10 MPa. [Color figure can be viewed in the online issue, which is available at wileyonlinelibrary.com.]

Figure 11 Plots of cell density of PMMA homopolymer and PMMA/PP blends at different PP content foamed at 100°C and 10 MPa. [Color figure can be viewed in the online issue, which is available at wileyonlinelibrary.com.]
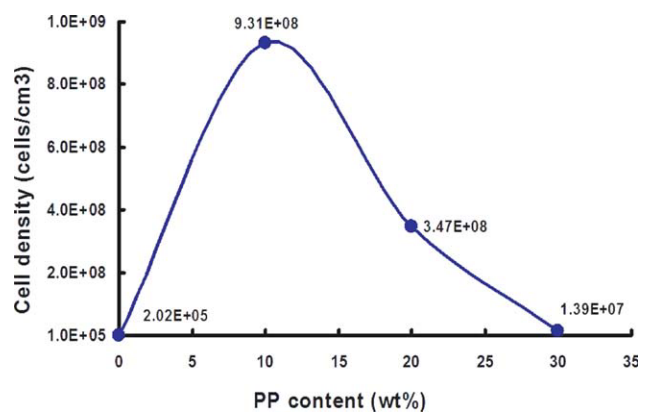
TABLE III
Interfacial tension of pairs of polymers

Polymers	Literature value (mN/m)
PP/PS	5.68
PP/PMMA	7.50
PS/PMMA	1.69

(2) In the case of $\gamma_A \geq \gamma_B + \gamma_{AB}$, the bubble nucleation occurs predominantly in polymer B and tends to detach from the interface.

(3) If both $\gamma_A < \gamma_B + \gamma_{AB}$ and $\gamma_B < \gamma_A + \gamma_{AB}$ hold, the bubbles mostly nucleate at the interface.

In this study, polymer A is PP, and polymer B represents either PS or PMMA, as shown in the schematic diagram of the bubble function at the interface between two immiscible polymers (see Fig. 12). Given the surface tension of PP to CO_2, γ_A is large at the foaming temperatures of 80 and 100°C because of the existence of the crystalline phase in PP, and the interfacial tension, γ_{AB}, is also large. Cases (2) and (3) can both be applied to PS/PP and PMMA/PP blends. In the case of the PS/PP blend, considering that CO_2-induced reductions of the sur-
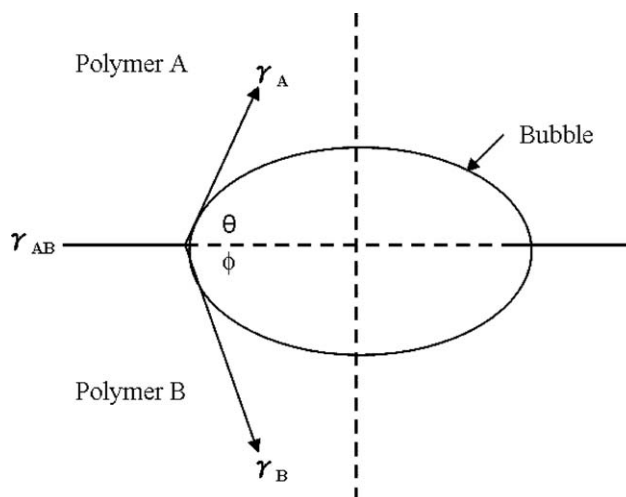

Figure 12 Schematic diagram of bubble formation at the interface of two immiscible polymers.

face tension of PP and PS in CO_2 at 170°C and 10 MPa[20] are 12 and 13 mN/m, respectively, bubbles are more likely to nucleate and become stable at the interface. The situation could hold for case (3). The larger the interfacial tension, γ_{AB}, is, the smaller the
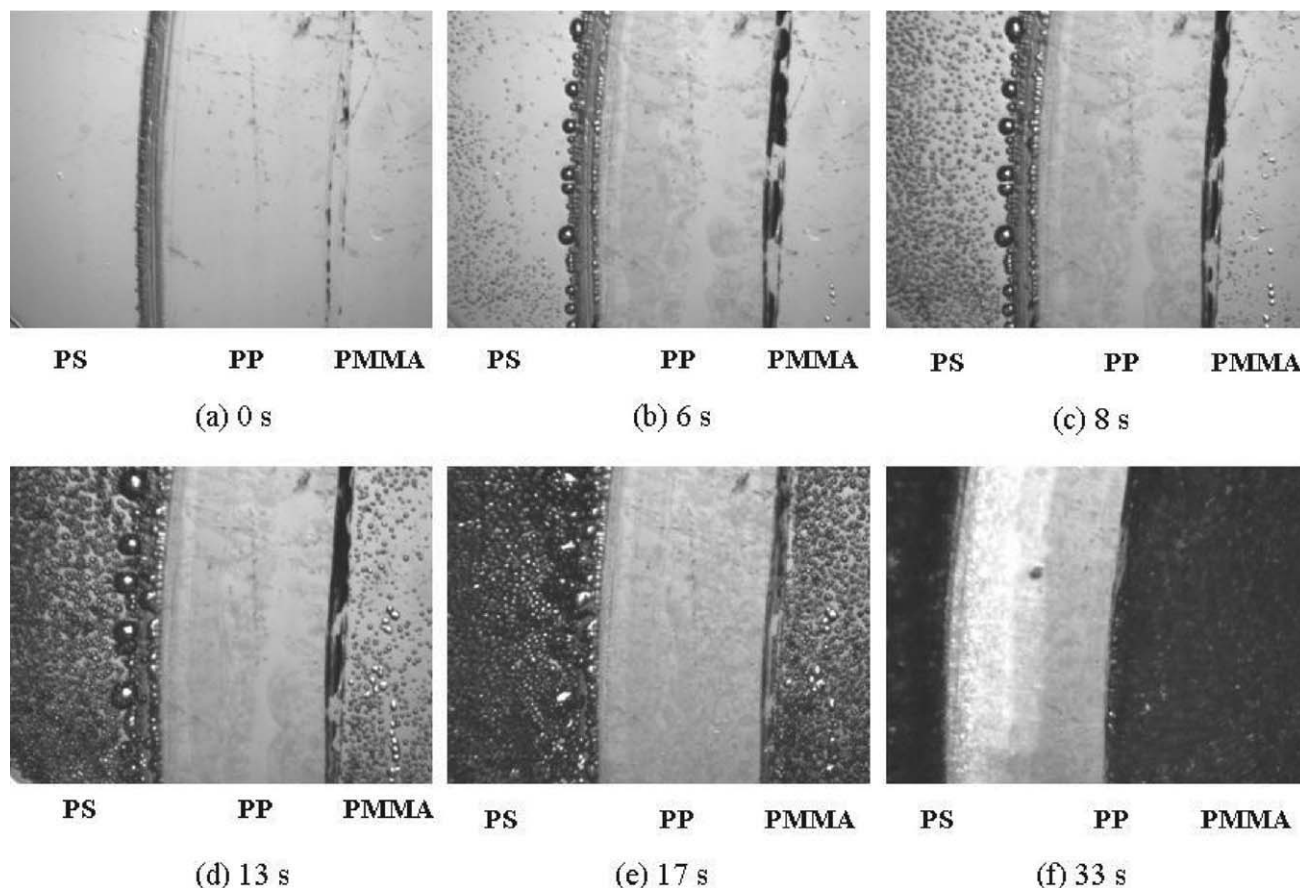

Figure 13 Bubble nucleation and expansion evolution processes of the PS/PP and PMMA/PP interfaces observed by visual observation experiment.

wetting angles, θ and ϕ, become. As a result, more bubbles are nucleated at the interface.

In the physical foaming, the following rule generally holds; the bubbles that nucleated earlier will grow faster and end up as larger cells. This mechanism with the aforementioned balance of three interfacial tensions at the interface created the void space around the PP domains in the PS as well as PMMA matrix. As listed in Table III, the interfacial tension between PMMA/PP is the largest among the three. Referring to the cell structure of the PMMA/PP (70/30) blend, which had the large void spaces around the PP domains [see Fig. 9(d–f)], it could be assumed that bubble nucleation occurs earlier at the interface between PMMA/PP, which is in line with the rule in case (3) condition. The larger void space around the domains in PMMA/PP compared with the PS/PP blend could be explained by this mechanism.

To confirm the bubble nucleation and growth behavior at the interface of the two polymers, a visual observation experiment was also conducted. The details of the experimental setup were given in our previous article.[21] The bubble nucleation and growth at the interface between PS and PP as well as PMMA/PP were observed by using a high-pressure view cell. Rectangular films of each polymer, PP, PS, and PMMA, were prepared and placed in parallel in the high-pressure view cell for the purpose of creating the interfaces of PS/PP and PMMA/PP.

The visual observation experiment was conducted by releasing the pressure from 10 MPa to atmospheric pressure within 48 s after dissolving CO_2 for 6 h at 150°C. Snapshot pictures were taken during the pressure quench foaming experiment as illustrated in Figure 13. Because of the limitation of the resolution of the high-speed camera, the smallest bubble that could be detected was 10 μm. Thus, the nuclei of bubbles below 10 μm could not be observed. During foaming, however, many bubbles were formed at the PP/PS and PMMA/PP interfaces. As time elapsed, dark portions appeared at the interface between PMMA/PP and expanded along the interface [Fig. 13(a)]. Then, the spherical bubbles appeared at the interface between PS and PP [Fig. 13(b)]. That is, the heterogeneous nucleation occurred first at the interface of PMMA/PP and later at the PS/PP interface. Subsequently, bubbles appeared in the PS and PMMA regions [Fig. 13(d,e)]. There was no bubble formation in PP during the course of foaming. This movie confirms that bubble nucleation is enhanced at the interface of two polymers. Furthermore, the interface with higher interfacial tension induces the heterogeneous nucleation and serves as a preferential site for bubble nucleation.

CONCLUSION

The cell structures of PS/PP and PMMA/PP blend foams were investigated. PP content could improve cell density and cell size over the homopolymers as long as PP had a small domain size and larger surface-to-volume ratio, and the foaming was conducted at a temperature lower than the melting temperature, T_m, of PP. The bubble nucleation could be enhanced at the interface of two polymers with higher interfacial tension. By manipulating the temperature and blend ratio, PP could be used as a nucleating agent with good dispersibility and high nucleating ability.

References

1. Tu, Z.; Mai, K.; Wu, Z. J Appl Polym Sci 2006, 101, 3915.
2. Han, X.; Shen, J.; Huang, H.; Tomasko, D. L.; Lee, L. J Polym Eng Sci 2007, 47, 103.
3. Colton, J. S.; Suh, N. P. Polym Eng Sci 1987, 27, 500.
4. Goel, S. K.; Beckman, E. J. AIChE J 1995, 41, 357.
5. Garcia, D. J Polym Sci Polym Phys Ed 1984, 22, 2063.
6. Lee, L. J.; Zeng, C.; Cao, X.; Han, X.; Shen, J.; Xu, G. Compos Sci Technol 2005, 65, 2344.
7. Zhai, W.; Yu, J.; Wu, L.; Ma, W.; He, J. Polymer 2006, 47, 7580.
8. Nam, P. H.; Maiti, P.; Okamoto, M.; Kotaka, T. Polym Eng Sci 2002, 42, 1907.
9. Taki, K.; Yanagimoto, T.; Funami, E.; Ohshima, M. Polym Eng Sci 2004, 44, 1004.
10. Taki, K.; Nitta, K.; Kihara, S.; Ohshima, M. J Appl Polym Sci 2005, 97, 1899.
11. Spitael, P.; Macosko, C. W.; Mcclurg, R. B. Macromolecules 2004, 37, 6874.
12. Ramesh, N. S.; Rasmusen, D. H.; Campbell, G. A. Polym Eng Sci 1994, 34, 1685.
13. Nemoto, T.; Takagi, J.; Ohshima, M. Macromol Mater Eng 2008, 293, 991.
14. Park, C. B.; Cheung, L. K. Polym Eng Sci 1997, 37, 1.
15. Luzinov, I.; Pagnoulle, C.; Jerome, R. Polymer 2000, 41, 3381.
16. Tomasko, D. L.; Burley, A.; Feng, L.; Yeh, S. K.; Miyazono, K.; Kumar, S. N.; Kusaka, I.; Koelling, K. J Supercrit Fluids 2009, 47, 493.
17. Calvao, P. S.; Yee, M.; Demarquette, N. R. Polymer 2005, 46, 2610.
18. Valera, T. S.; Morita, A. T.; Demarquette, N. R. Macromolecules 2006, 39, 2663.
19. Hartland, S. Surface and Interfacial Tension: Measurement, Theory and Applications; Marcel Dekker Inc: New York, United States of America, 2004.
20. Taki, K.; Murakami, T.; Ohshima, M. Presented at the Proceedings of Asian Workshop of Polymer Processing, Singapore, 2002.
21. Ohshima, M.; Taki, K.; Nakayama, T.; Yatsuzuka, T. J Cell Plast 2003, 39, 155.